Imaging Agents

DOI: 10.1002/anie.200702167

Photochromic Rhodamines Provide Nanoscopy with Optical Sectioning**

J. Fölling, V. Belov, R. Kunetsky, R. Medda, A. Schönle, A. Egner, C. Eggeling, M. Bossi, and S. W. Hell**

Since the seminal work of Abbe in 1873, it has been commonly assumed that the resolution of a lens-based (far-field) light microscope is limited to about half the wavelength of the light used ($\approx\lambda/2$).[1] However, in the mid-1990s, fluorescence microscopy concepts emerged that demonstrated that the limiting role of diffraction could be fundamentally overcome. The main hallmark of these concepts was to use the states of the fluorescent marker not just for generating the signal, but also for breaking the diffraction barrier. In fact, all the methods that have successfully outperformed diffraction have so far relied on selected pairs of molecular states—specifically, a "bright" one to generate the signal and a "dark" one to ensure that the measured signal stems from a subdiffraction-sized region. For example, stimulated emission depletion microscopy[2] relies on the quenching of the fluorescent singlet state to the (dark) ground state by using a focal intensity distribution featuring a zero. Thus, all molecules are "switched off" except those located at the position of the zero. This concept has been successfully extended to switching between (metastable) states of fluorescent proteins[3,4] and photochromic organic compounds.[3,5] In this case, the switching occurs between (conformational) states, in one of which the molecule is able to successively emit fluorescence photons. The benefit is that the switching can be performed at low levels of light.

An alternative way of using molecular photoswitching to break the diffraction barrier is to stochastically switch on, read out the fluorescence, and switch off isolated marker molecules such that simultaneously emitting ("on") markers are further apart than the minimal distance resolved by the microscope. In this case, the spatial confinement of the fluorescence is down to the size of a single molecule by definition. Imaging the fluorescence signal from an individual marker onto a camera produces a diffraction spot whose centroid yields the location of the emitter, with a precision that ideally depends just on the number of collected photons n and on the full-width-half-maximum (FWHM) of the fluorescence spot,[6] and is approximately given by FWHM/$\sqrt{n}$. After being recorded, the molecules must go back to a dark state so that one is readily able to read out and calculate the centroid of an adjacent one. Repeating this procedure for a multitude of markers reconstructs their distribution with sub-$\lambda/2$ resolution. The main advantage of this single-molecule read-out strategy (known as PALM,[7] STORM,[8] and fPALM[9]) over the zero-intensity-based read-out mode (RESOLFT) is that the marker molecules are not forced to undergo several photoswitching cycles. On the other hand, new requirements and limitations are introduced. The fluorescent "on" state must yield enough photons to allow the precise calculation of the centroid. At the same time, the single-molecule approach requires a strict control over the maximum density of photoactivated molecules, and it also depends on their reliable localization against a diffuse background. Therefore, a finite contrast in brightness between the "on" and "off" states as well as the spontaneous activation of molecules during fluorescence read-out restrict this approach to thin samples with a low fluorophore concentration.

Herein, we report a new photochromic rhodamine derivative that has allowed us to overcome these limitations. This readily controllable photoswitchable compound has a high fluorescence quantum yield and high photochemical stability under single-molecule conditions. The resulting dramatic increase in n yields an average localization precision of approximately 10 nm. In conjunction with an optimized asynchronous image acquisition protocol, the large contrast between the two photochromic states involved minimizes the diffuse background and allows us to abandon the total internal reflection (TIRF) recording schemes and mechanical object slicing that were mandatory in previous experiments.[7,8] At the same time, it allows us to operate with a higher density of detectable markers per unit volume. Moreover, our compound can be switched on by two-photon absorption, thereby restricting the process to the focal plane. The method can therefore be applied to the imaging of selected individual layers inside thick three-dimensional samples.

Thus, the improved photochemical properties of the compounds now allow us to report far-field optical nanoscopy by single-molecule switching with non-invasive optical sectioning.

[*] Dipl.-Phys. J. Fölling, Dr. V. Belov, Dipl.-Chem. R. Kunetsky, Dipl.-Biol. R. Medda, Dr. A. Schönle, Dr. A. Egner, Dr. C. Eggeling, Dr. M. Bossi, Prof. Dr. S. W. Hell
Abteilung NanoBiophotonik
Max-Planck-Institut für Biophysikalische Chemie
Am Fassberg 11, 37077 Göttingen (Germany)
Fax: (+49) 551-201-2506
E-mail: mbossi@gwdg.de
shell@gwdg.de
Homepage: http://www.mpibpc.gwdg.de/abteilungen/200/

[**] This work was supported by the European Commission through a SPOTLITE grant to S.W.H. and a Marie Curie Fellowship to M.B., and a BMBF program (Biophotonics) grant. We thank C. Geisler and B. Rankin for helpful assistance.

Supporting information for this article is available on the WWW under http://www.angewandte.org or from the author.

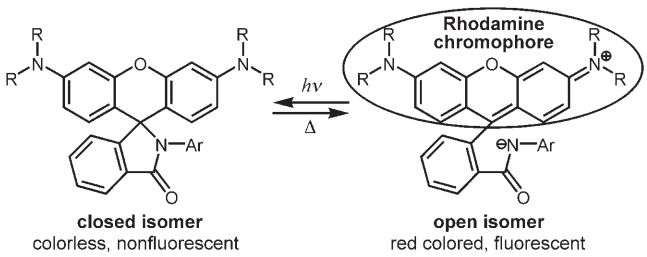

Scheme 1. Photochromic reaction of rhodamine derivatives with light-induced activation ($h\nu$) of fluorescence (open isomer) and thermal relaxation (Δ) to the deactivated state (closed isomer).

A photochromic reaction of rhodamine amides was reported in the 1970s by Knauer and Gleiter[10] (Scheme 1), but was almost disregarded in the following years—perhaps because of the low quantum efficiency of the photoinduced reaction, the low thermal stability of the open isomer that has a lifetime of a few milliseconds in polar solvents,[11] or the low number of repetition cycles available per molecule. These are commonly treasured features of photochromic compounds for applications, such as optical memories and switches.[12]

However, these compounds have excellent properties for markers in single-molecule microscopy (Figure 1 and Scheme 2). Rhodamine B (R = Et), which was selected for the construction of derivatives **5**-R (Scheme 2), is a highly stable fluorescent dye. 4-Aminophthalimide was selected as the aryl substituent to provide a significant absorption in the near-UV region, and a linking point (the imide nitrogen atom) was chosen for further functionalization. The electron-acceptor group (one carbonyl group is directly conjugated with the negatively charged nitrogen atom in the open form) should also help to stabilize the charge at the amide nitrogen atom in the open isomer and to improve the photoactivation process. The blue fluorescence of free amine **3** (Scheme 2), typical for aminophthalimides, disappears after acylation.

The photoinduced switch-on reaction of **5**-R derivatives results in the generation of the chromophore of the rhodamine dyes (Scheme 1) which absorbs in the green region and emits at around 580 nm. The closed isomer is transparent in the visible range (Figure 1) and is practically nonfluorescent. Note that the extended conjugation in the three condensed cycles is broken in the closed isomer, thus rendering a huge contrast between the signals of the two states. Besides having the fluorescence spectral properties of an *N*-aryl-substituted rhodamine,[13] the open isomer of **5**-R is brightly fluorescent and can be imaged at the single-molecule level with an average of up to 900 photons detected per molecule in polyvinylalcohol (PVA; Figure 2). The open isomer spontaneously (Δ) reverts to the thermodynamically stable closed

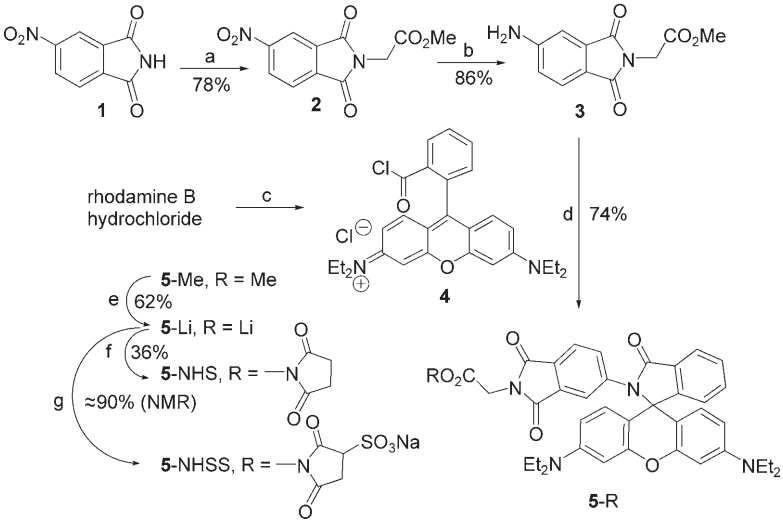

Scheme 2. Synthetic route for the preparation of compounds **5**-R: a) $BrCH_2CO_2Me$, *t*BuOK, DMF, 40 °C, 24 h; b) H_2, Pd/C, THF, room temperature and pressure, 4 h; c) $POCl_3$, 1,2-dichloroethane, reflux, 4 h; d) MeCN, Et_3N, reflux, 24 h; e) LiI (3 equiv), EtOAc, reflux, 24 h; f) 2-succinimido-1,1,3,3-tetramethyluronium tetrafluoroborate, DMF, RT, 2 h; g) *N*-hydroxysulfosuccinimide sodium, *O*-(7-azabenzotriazol-1-yl)-*N*,*N*,*N*′,*N*′-tetramethyluronium hexafluorophosphate (HATU), DMF, RT, overnight.

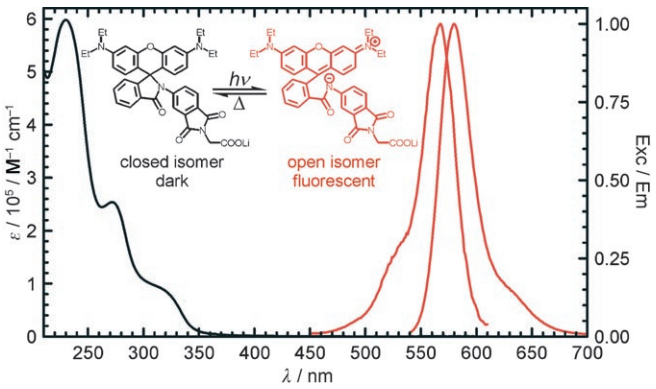

Figure 1. Absorption spectra of **5**-Li (closed isomer, black line, left axis) in water solution, and excitation and emission spectra of the open isomer in a PVA film after photoactivation with 366-nm light (red lines, right axis; detection: 620 nm; excitation: 530 nm).

isomer, with a kinetic constant that strongly depends on the solvent (milliseconds in polar solvents; up to hours in PVA).[11] Conversely, thermal activation to the open "on" state is marginal for **5**-Li. A fraction of $1/10^4$ spontaneously activated molecules was measured in single-molecule experiments in a PVA film, after a relaxation time in the dark to allow the sample to reach thermal equilibrium. The key to the high fluorescence observed in the open isomer of photochromic rhodamine amides is the absence of a photoinduced back reaction (open→closed isomer) which also eliminates an undesirable competition between read-out and switch-off.

The **5**-R derivatives have all the necessary properties for superresolution microscopy by switching single fluorescence emitters: 1) switching with a large contrast between the fluorescence signals of the on and off states, 2) a low fraction of spontaneously activated on-state markers, and 3) a high number of emitted photons n in the on state. Figure 2

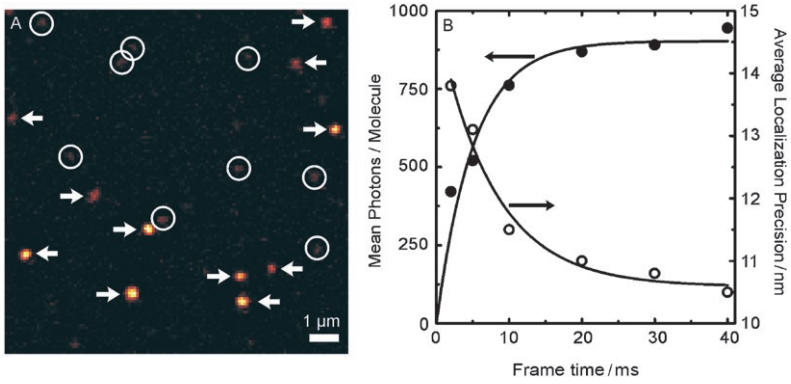

Figure 2. A) Single-molecule imaging of a PVA film containing 1.3×10^6 **5**-Li molecules μm^{-2} after switching them on with 50 $W cm^{-2}$ of 375-nm light (excitation wavelength 532 nm, 18 $kW cm^{-2}$). Localized molecules are indicated with arrows, while the circled ones were rejected because of the low number of photons (typical rejection threshold: 200 photons). B) Average number of photons detected per single molecule per frame as a function of the CCD frame time for the same sample, and the corresponding localization precision for an instrumental point spread function of 270 nm FWHM.

illustrates these three qualities. Figure 2A shows a typical CCD image recorded from a PVA film containing a high density of markers (1.3×10^6 molecules μm^{-2}), where only a few are in the emitting state. As can be observed, hardly any background fluorescence arises from the large number of markers in the off-state, clearly identifying single fluorescing **5**-Li molecules. In our experiments, we used an acquisition mode referred to as PALMIRA (PALM with independently running acquisition): single-molecule image snapshots as shown in Figure 2A are continuously recorded with a frame time matched to the average on-time of single fluorophores before they are irreversibly bleached or thermally deactivated. Figure 2B shows the mean number of photons n that can be extracted per molecule from a single frame as a function of the exposure time and at a fixed excitation power. The excitation power was chosen for an optimized duty cycle of the rhodamine dye; it is close to the saturation value of the fluorescence emission.[14] The value of n increases with exposure time until it reaches its maximum value of about 900 photons at times larger than 20 ms. The expected average precision of single-molecule localization, given approximately by FWHM/$\sqrt{n}$, which determines the resolution in the final image, improves from about 14 nm in the case of an exposure time of 2 ms down to about 10.5 nm at exposure times greater than 20 ms. Matching the frame time to the average on-time of our fluorophore of approximately 10 ms ensures close to optimal localization accuracy while minimizing the background fluorescence. Frame times greater than 10 ms give slightly better accuracy but increase the acquisition time ($\approx$ frame time $\times$ number of frames) and the background signal. Shorter frame times reduce the localization precision because they spread the same single-molecule event over several frames and lead to a larger contribution of the read-out noise. We were able to collect enough single-molecule events to form meaningful images in 10000 to 20000 frames, thus resulting in acquisition times of only 1–3 minutes for a total image. Our setup proved sufficiently stable during this short period. Therefore, neither mechanical stabilization nor compensation for drift or vibration was needed in any of the measurements.

Our experiments were performed in PVA where the lifetime of the open isomer is on the order of hours. Since the reversibility of the process can be neglected on this timescale, the dye behaves as a typical caged fluorescent compound: it is activated, imaged, and then bleached. Therefore, the saturation value reached in Figure 2B is determined by photoinduced bleaching. In combination with our continuous asynchronous readout mode, an advantage of this irreversible deactivation of the **5**-R derivatives is that a thermal equilibrium of the activation reaction is not reached between frames. Thus, the fraction of molecules that are in the emitting state as a result of spontaneous activation is lower than those in equilibrium ($1/10^4$), thus allowing single molecules to be individually detected within the instrument's resolution limit in samples with a marker density of about 10^7 molecules μm^{-2} (Figure 2A). The thermal relaxation takes place in about 20–100 ms in polar solvents.[11] By introducing a lag-time in between frames to allow for this relaxation, it could therefore be used to localize markers several times, thereby allowing for multiple measurements on the same sample, which is an advantage for future dynamic (live-cell) experiments.

A tubular network of mammalian PtK2 cells labeled with **5**-NHSS and mounted in mowiol was imaged in our microscope by using wide-field photoactivation with light of a wavelength of 375 nm. For highly dense immunostained samples, the first 100–1000 images could be measured with no photoinduced activation by using the few spontaneously activated molecules. The dose of the activating light was then increased with the number of acquired frames, as the number of remaining markers decreased. The typical exposure time for a single frame was between 2 and 10 ms with an excitation power (532 nm) of 18 $kW cm^{-2}$ in the focal plane. Figure 3 shows reconstructed images[15] of tubulin filaments from 10240 CCD frames (total acquisition time: 108 s). The improvement in the spatial resolution achieved with single-molecule photoswitching over conventional wide-field epifluorescence imaging is demonstrated with single filaments. For a fair comparison, we have linearly deconvolved the latter. The size of a single filament is about 55–70 nm, in agreement with the value expected from the filament itself with a diameter of approximately 25 nm plus the primary and secondary antibodies used for labeling. The average number of photons detected per molecule in the cell environment was about 850,[15] which, according to Figure 2B, renders an average localization accuracy of about 11 nm.

Switching on the dyes (Scheme 1) can be either performed in the one-photon-absorption (1PA) regime with UV light in the wavelength range 313–380 nm, or with two-photon absorption (2PA) using red light of wavelength 650–800 nm. In the second case, fast imaging relies on high intensities that can be achieved through focusing short pulses. To this end, we

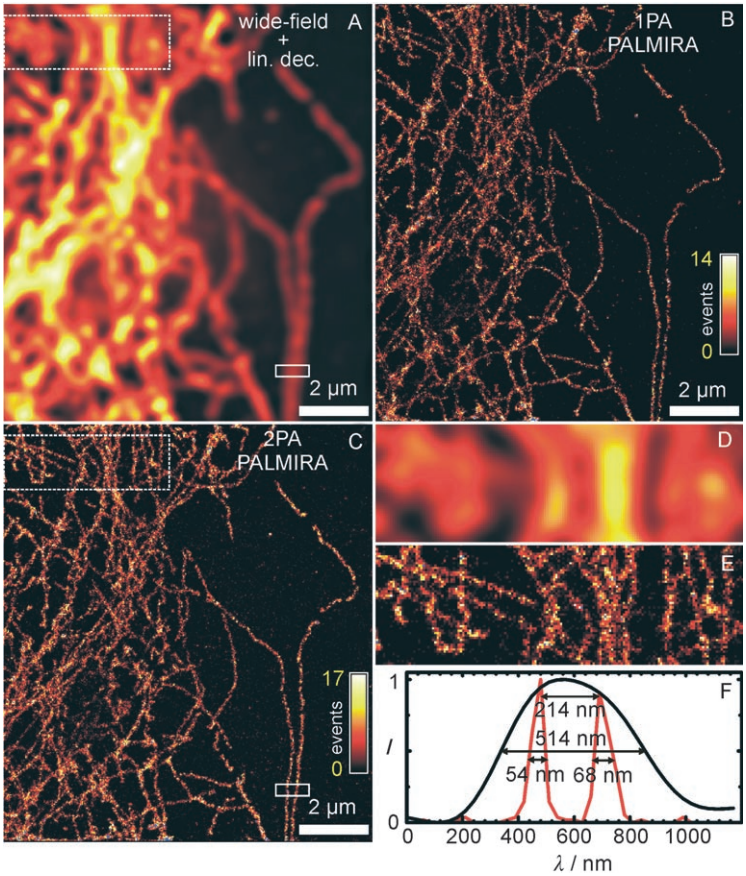

Figure 3. Reconstructed images of the tubulin network in a PtK2 cell stained with **5**-NHSS. A) Wide-field image; B) one-photon (375 nm) 1PA-PALMIRA image; C) two-photon (747 nm) 2PA-PALMIRA image. D, E) enlarged sections from (A) and (C), respectively (dotted-line boxes). F) Profiles across the *x* direction of two adjacent filaments, averaged in the *y* direction (full-line box in (A) and (C)), from the wide-field (black line) and 2PA-PALMIRA (red line) images.

constantly scanned the pulsed 2PA beam (747 nm) over the whole image area during the acquisition to install the desired level of "on" molecules in the field of view. The 2PA-PALMIRA image (20480 CCD frames at 10 ms exposure time) of the tubulin filaments is also displayed in Figure 3; it is virtually identical to that obtained with one-photon activation (1PA). The same image construction process was used for the data acquired with 1PA and 2PA.[15] The image acquisition time with 2PA was technically limited by the speed of the scanning system (30 Hz), but can in principle be accelerated. There is no fundamental reason why 2PA could not be as fast as 1PA.

Several advantages emerge from the use of 2PA over 1PA. UV light may induce sample damage and lead to autofluorescence, while red light minimizes these effects. The most important difference is that 2PA is only effective in a thin plane,[16] thus providing optical sectioning. To demonstrate the sectioning capability, 5 µm amino-modified silica beads, surface-stained with **5**-NHSS were imaged using 2PA at different *z* positions with a typical spatial separation of 330 nm between slices. Figure 4 A shows a 3D reconstruction from 17 slices. Note the high lateral resolution obtained in the equatorial slice (Figure 4 B) with a practically zero background contribution from out-of-plane molecules.

To illustrate the feasibility of 2PA-PALMIRA with axial sectioning in cell biology, we imaged lamin proteins stained with **5**-NHSS in the nucleus of human glioma cells. The nuclear lamina is clearly observed (Figure 4 C). Note the tubelike connection of the surfaces in the foreground which is characteristic of the lamin skeleton of the nucleus. An excellent lateral resolution was achieved (Figure 4 D), even in this thick sample (> 6 µm), thus showing the viability of imaging in whole cellular environments without the need for further treatments such as (cryo)sectioning.

In conclusion, we have introduced a chemical marker for fluorescence nanoscopy that relies on single-molecule photoswitching. Based on the photochromism of rhodamine amides, this novel marker allowed for a range of important advancements in subdiffraction-resolution imaging. The new fluorophore emits a large number of photons per on-time which provides a high spatial resolution. A high contrast between the emitting and the dark isomers, and inhibition of spontaneous transitions to the on state enable the generation of detailed images from thick and densely stained samples. Rhodamine amides can be switched on

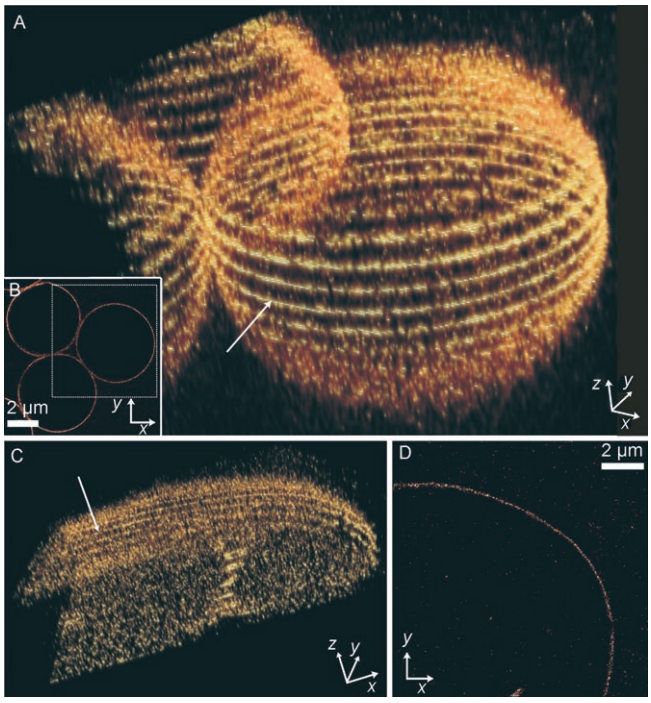

Figure 4. A, B) 2PA-PALMIRA imaging of 5-µm silica beads surface-stained with **5**-NHSS. A) 3D reconstruction from 17 slices in the *z* direction; B) equatorial slice (arrow in (A)). For clarity, a smaller area was selected for the 3D reconstruction (dotted-line box in (B)). C, D) 2PA-PALMIRA imaging of lamin of a U373MG cell stained with **5**-NHSS. C) 3D reconstruction from 10 slices in the *z* direction. D) Equatorial slice (arrow in (C)).

using two photons, thus providing for the first time axial optical sections of 0.5–1 μm—a fundamental improvement over 1PA, which offers virtually no axial discrimination. Extending the applicability of single-molecule-based nanoscopy beyond single layers opens up the prospect of 3D imaging of living cells. In the future, 2PA combined with maximum-likelihood procedures for axial localization[17] will result in improved axial resolution. Since the emission spectrum of our compound is easily shifted by changing the rhodamine, we also anticipate multicolor applications using a single light source for switching on the emission of various fluorescence molecules.

Experimental Section

Synthesis of the fluorescent probes:[15] Compound **3** was prepared from 4-nitrophtalimide (**1**) and acylated with rhodamine B acid chloride (**4**, Scheme 2). Cleaving the methyl ester with LiI in refluxing ethyl acetate[18] afforded the lithium salt **5**-Li, which was further used for the preparation of *N*-hydroxysuccinimidyl esters **5**-NH(*S*)S. They react readily with N-terminal amino groups and *ω*-amino residues of lysines in proteins. *N*-Hydroxysulfosuccinimidyl derivative **5**-NHSS is soluble in water, and, therefore, it was used for staining (without isolation from the reaction mixture, in which it had been formed in high yield).

PALMIRA microscope: We employed a home-built wide-field microscope with a two photon beam scanning system. 1PA light (375 nm) was delivered by a diode laser (iPulse-375, Toptica Photonics AG, Gräfelfing, Germany) and the circularly polarized excitation light (532 nm) by a DPSS laser (VERDI V10, Coherent Inc., Santa Clara, CA, USA). Both beams were focused into the back aperture of the objective lens (PL APO 100×, 0.7–1.4, Leica Microsystems, Wetzlar, Germany) to provide wide-field illumination (ca. 12 μm FWHM) with a mean intensity in the focal plane of 18 kW cm^{-2} for the 532 nm and 50 W cm^{-2} for the 375 nm light (pulses of up to 500 μs). 2PA light (747 nm) was provided by a Ti:Sa laser (Mira 900, Coherent Inc.) coupled to a hollow core fiber with low dispersion (AIR-6-800, Crystal Fibre A/S, Birkerød, Denmark), characterized by a pulse length of 5 ps (76 MHz repetition rate) and a diffraction-limited focal spot of 280 nm FWHM. A resonant mirror (EOPC, Glendale, NY, USA) and an independently running piezo-actuated mirror (PSH 5/2 SG, Piezosystem Jena, Germany) were used for the fast (14.6 kHz) and the slow axis (30 Hz) of the 2PA scanning system, respectively.

Fluorescent light was collected by the same objective, separated from the activation and excitation beams by means of a dichroic mirror and bandpass filters, and imaged onto an EM-CCD camera (IXON-Plus DU-860, Andor Technology, Belfast, Northern Ireland). A custom-made sample holder based on a manual Microblock 3-Axis Positioner (Thorlabs, Newton, NJ, USA) was used. The fine positioning of the focal plane in the sample was achieved with a *z*-axis objective lens positioner (MIPOS 4 CAP, Piezosystem Jena).

Received: May 16, 2007
Published online: July 19, 2007

Keywords: dyes/pigments · fluorescence · microscopy · photochromism · photoswitchable compounds

[1] E. Abbe, *Arch. f. Mikr. Anat.* **1873**, *9*, 413–420.
[2] S. W. Hell, J. Wichmann, *Opt. Lett.* **1994**, *19*, 780–782.
[3] S. W. Hell, S. Jakobs, L. Kastrup, *Appl. Phys. A* **2003**, *77*, 859–860.
[4] M. Hofmann, C. Eggeling, S. Jakobs, S. W. Hell, *Proc. Natl. Acad. Sci. USA* **2005**, *102*, 17565–17569.
[5] M. Bossi, J. Fölling, M. Dyba, V. Westphal, S. W. Hell, *New J. Phys.* **2006**, *8*, 275.
[6] W. E. Moerner, *Nat. Methods* **2006**, *3*, 781–782.
[7] E. Betzig, G. H. Patterson, R. Sougrat, O. W. Lindwasser, S. Olenych, J. S. Bonifacino, M. W. Davidson, J. Lippincott-Schwartz, H. F. Hess, *Science* **2006**, *313*, 1642–1645.
[8] M. J. Rust, M. Bates, X. Zhuang, *Nat. Methods* **2006**, *3*, 793–796.
[9] S. T. Hess, T. P. K. Girirajan, M. D. Mason, *Biophys. J.* **2006**, *91*, 4258–4272.
[10] K. H. Knauer, R. Gleiter, *Angew. Chem.* **1977**, *89*, 116–117; *Angew. Chem. Int. Ed. Engl.* **1977**, *16*, 113–113.
[11] H. Willwohl, J. Wolfrum, R. Gleiter, *Laser Chem.* **1989**, *10*, 63–72.
[12] *Molecular Switches* (Ed: B. L. Feringa), Wiley-VCH, Weinheim, **2001**.
[13] T. Nguyen, M. B. Francis, *Org. Lett.* **2003**, *5*, 3245–3248.
[14] C. Eggeling, J. Widengren, R. Rigler, C. A. M. Seidel, *Anal. Chem.* **1998**, *70*, 2651–2659.
[15] See the Supporting Information for details.
[16] W. Denk, J. H. Strickler, W. W. Webb, *Science* **1990**, *248*, 73–76.
[17] F. Aguet, D. Van De Ville, M. Unser, *Opt. Express* **2005**, *13*, 10503–10522.
[18] J. W. Fisher, K. L. Trinkle, *Tetrahedron Lett.* **1994**, *35*, 2505–2508.

